

ORIGINAL ARTICLE

# Comparison between DSC and TMDSC in the investigation into frozen aqueous cryoprotectants solutions

A. Santoveña, M.J. Piñero and M. Llabrés

*Departamento de Ingeniería Química y Tecnología Farmacéutica, Facultad de Farmacia, Universidad de La Laguna, La Laguna, Tenerife, Spain*

---

## Abstract

**Purpose:** The influence of thermal parameters in the observation of thermal events and in the calculation of heat transformation in aqueous cryoprotectant solutions after freezing was investigated using conventional differential scanning calorimetry (DSC) and temperature-modulated DSC (TMDSC), respectively. **Methods:** The systems under study were formed by pure water and diluted aqueous solutions of mannitol, trehalose, sucrose, sorbitol, and glycine. The influence of different combinations of frequency and amplitude was analyzed in heating-cooling and heating-iso TMDSC scans. **Results:** Trehalose, sucrose, and sorbitol present a lesser critical temperature of primary drying than other cryoprotectants studied. The calorimetric variables selection is crucial to detect or not the thermal events, or to detect so with different numerical values. Then, the values of the calorimetric parameters determined are different if measured in a mode of heating-cooling or heating-iso. The TMDSC method-1 used in this study employs a higher number of cycles in each thermal event. The use of Lissajous figures and the study of the  $C_{p \text{ in-phase}}$  signal evolution will allow us to understand the complexity of the events detected. **Conclusions:** The comparative study of both techniques points to the selection of conventional or modulated technique depending on the type of system and the nature of the studied events.

**Key words:** Cryoprotectants; crystallization; differential scanning calorimetry; melting; phase transition; temperature-modulated differential scanning calorimetry

---

## Introduction

Cryoprotectants are substances used to protect biological tissues from freezing damage. These agents stabilize and prevent the degradation of drugs during freeze-drying and storage. Materials to be freeze-dried are usually complex mixtures of solute in solutions that form eutectic and glassy amorphous masses upon freezing. The use of cryoprotectants will stabilize bioproducts against harmful freezing effects by reducing undesirable ice crystal formation and solute concentration effects and by increasing amorphous mass structure. The freezing process may be evaluated and monitored by a number of techniques that include differential scanning calorimetry (DSC), differential thermal analysis, freeze-drying microscopy, and resistivity measurements<sup>1</sup>.

Since its introduction as a basic calorimetric technique, the DSC has been widely employed in pharmaceutical research, preformulation and drugs polymorphs and excipients characterization<sup>2–7</sup>, compatibility assays between drugs and excipients<sup>8–11</sup>, investigation of the freezing process previous to lyophilization<sup>12,13</sup>, and in the stability assays of protein drugs<sup>14–16</sup>. Some of the difficulties that appear during the DSC thermograms interpretation are due to the measured magnitude and the total heat flow formed by the two components: one due to the sensible heat of the sample, proportional to its specific heat capacity, and other that represents the heat flow caused by physical or chemical transformation processes.

The temperature-modulated differential scanning calorimetry (TMDSC) was initially developed by Reading in 1993<sup>17</sup> with the aim of separating the total heat flow

---

Address for correspondence: A. Santoveña, Ph.D., Departamento de Ingeniería Química y Tecnología Farmacéutica, Facultad de Farmacia, Universidad de La Laguna, 38200 La Laguna, Tenerife, Spain. Tel: +34 922 316502, Fax: +34 922 318506. E-mail: ansanto@ull.es

(Received 5 Oct 2009; accepted 10 Apr 2010)

ISSN 0363-9045 print/ISSN 1520-5762 online © Informa UK, Inc.  
DOI: 10.3109/03639045.2010.487264

<http://www.informapharmascience.com/ddi>

in reversing and nonreversing components. Because the TMDSC has allowed solving usual problems of drugs preformulation field<sup>18–21</sup>, this has taken the place of DSC in this investigation area over the last years. An example of this is the TMDSC monographic volume edited by *International Journal of Pharmaceutics* in 1999<sup>22</sup>, specially the work of Verdonck et al.<sup>23</sup> about the basis of this technique. In TMDSC, a periodically modulated temperature is superimposed on the linear temperature program used in conventional DSC, separating the total heat flow in reversing and nonreversing components. Thus, the TMDSC has allowed obtaining additional information about different types of process, such as glass transition ( $T_g$ ) and degradation of drugs and excipients, compatibility between different elements of a pharmaceutical formulation, significant events in the preformulation steps of a drug, and so on.

However, in the last years, it has been checked that the use of TMDSC and the interpretation of the thermograms are more complicated than it had been originally supposed. This ambiguity has been partly due to the wide variety of commercial equipments available, each of which offered slightly different modulated temperature profiles and/or slightly different procedures for the analysis of data<sup>24</sup>.

Although there are few documents in the scientific literature, which complement both techniques to study different types of thermal events<sup>20,25–28</sup>, this work is focused on carrying out a comparative study of the same thermal events obtained by DSC and TMDSC and on making the selection of the calorimetric variables of each method in the observation of different processes (first- and second-order phase transitions) obtained after freezing aqueous cryoprotectants solutions frequently used in the preformulation of drugs.

## Materials and methods

### Materials

All samples were prepared with distilled and deionized water by a Milli-Q<sup>®</sup> system (Millipore Iberica, Spain). Mannitol (Avocado<sup>®</sup>, batch D9793A), trehalose (Panreac<sup>®</sup>, batch 1456DKR), sucrose (Sigma<sup>®</sup>, batch G1K00611), sorbitol (Acofarma<sup>®</sup>, batch 020219S-7), and glycine (Merck<sup>®</sup>, batch 8532101) were used as cryoprotectants substances. The samples were diluted to the limit of its solubility with distilled and deionized water. The crucibles

(pans) used were of aluminum with pin and 40  $\mu$ L capacity (Mettler Toledo<sup>®</sup>).

### Methods

All experiments were carried out with a DSC Mettler Toledo 821<sup>e</sup> equipment with STAR<sup>e</sup> software option (Greifensee, Switzerland), which allows us to work with conventional DSC or with TMDSC. The calorimeter was calibrated in temperature and heat with indium and zinc as standards.

The samples analyzed with conventional DSC were kept at  $-50^\circ\text{C}$  for 10 minutes and then, they were heated up to  $25^\circ\text{C}$  with a rate of  $1^\circ\text{C}/\text{min}$  in an atmosphere of nitrogen gas at a flow of 100 mL/min. Every sample was analyzed in triplicate.

The samples analyzed with TMDSC were subjected to thermal programs conditioned by the available software. The alternating DSC evaluation of STAR<sup>e</sup> software is obtained after marking and processing the blank measurement, calibration curve, and sample curve of each sample. This evaluation is based on thermal analysis principles with additional calibration, and therefore the evaluations result in the absolute values for the reversing and nonreversing part of a periodical measuring curve. The reversing part is also given as specific heat capacity and its complex value is divided into two more curves:  $C_{p \text{ in-phase}}$  and  $C_{p \text{ out-phase}}$ , and the phase-angle is always shown. The weight difference was less than 20  $\mu\text{g}$  between sample and reference pan. Samples were analyzed in duplicate.

Table 1 shows the different TMDSC thermal methods used. Figure 1 shows the evolution in time of temperature and heating rate for each TMDSC method employed.

In DSC thermograms interpretation, the linear temperature  $T(t)$  increases in time  $t$  from an initial temperature  $T_0$  as

$$T(t) = T_0 + \beta_0 t. \quad (1)$$

Then the heating rate is a constant value equal to  $\beta_0$  and the heat flow is formed by three components,

$$\Phi(T, t) = \Phi_0(T, t) + \Phi_{Cp}(T, t) + \Phi_r(T, t). \quad (2)$$

**Table 1.** Calorimetric characteristics of thermal methods employed in TMDSC.

Method	Initial conditions ( $^\circ\text{C}/10 \text{ min}$ )	$\beta_0$ ( $^\circ\text{C}/\text{min}$ )	Amplitude ( $^\circ\text{C}$ )	Period (minutes)	$N_2$ (g) (mL/min)
1	$-50$	1.00	1.00	1.00	100
2	$-50$	1.00	0.16	1.00	100
3	$-50$	1.00	1.00	2.00	100

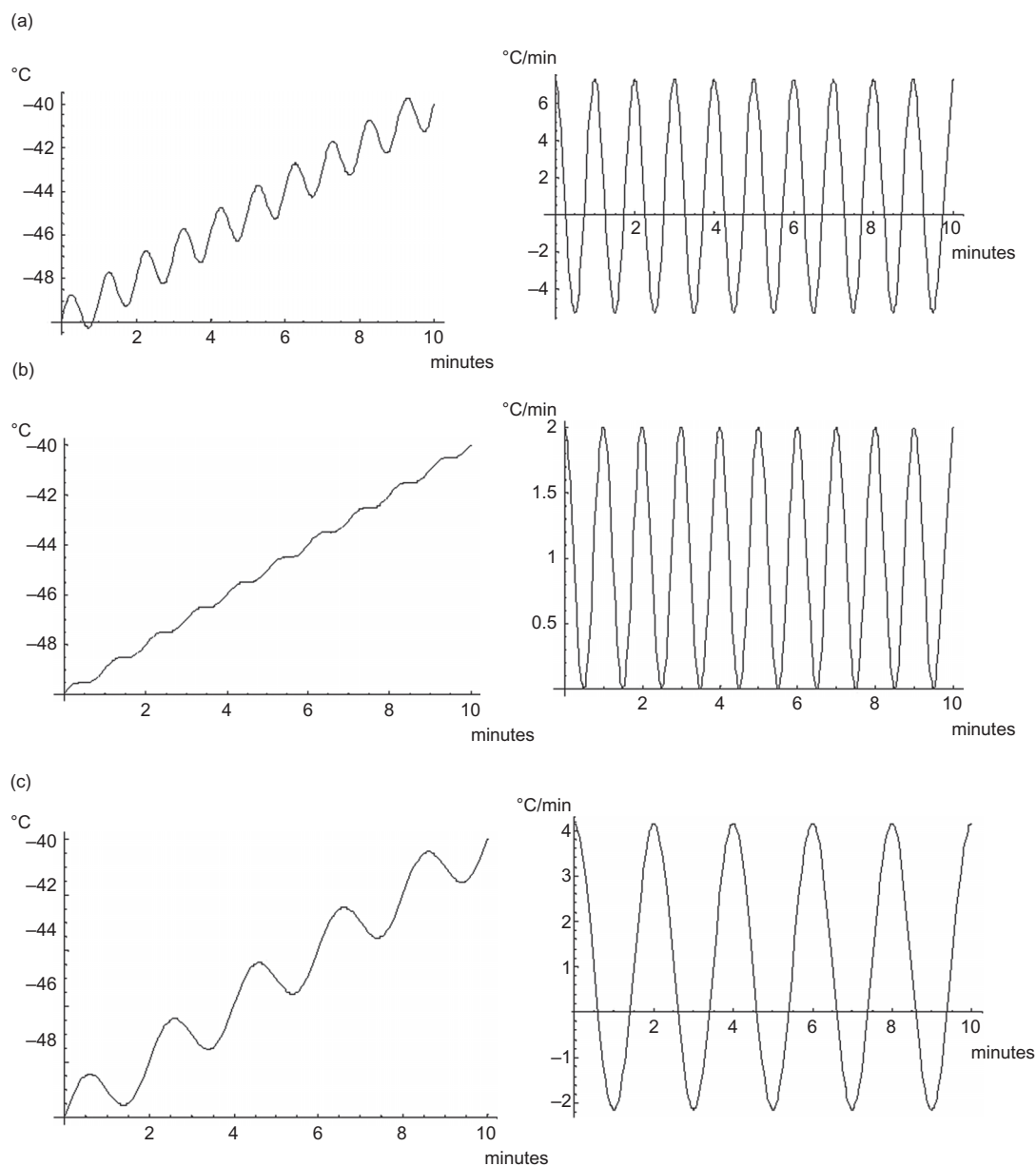


**Figure 1.** Evolution in time of temperature and heating rate of every TMDSC method employed: (a) method-1, (b) method-2, and (c) method-3.

$\Phi_0(T, t)$  is the factor that corrects the instrument asymmetry,  $\Phi_{cp}(T, t)$  is the heat flow due to the sample heat capacity ( $C_p$ ) the so-called sensible heat flow, and  $\Phi_r(T, t)$  corresponds to the latent heat flow caused by chemical reactions or phase transitions. In TMDSC, the linear temperature program of the DSC was superimposed with a sinusoidal temperature fluctuation,

$$T(t) = T_0 + \beta_0 t + A \sin(\omega t), \quad (3)$$

with  $\beta_0$  the underlying heating-cooling rate,  $A$  the temperature fluctuation amplitude, and  $\omega$  the angular

frequency modulation, related to the modulation period  $\tau$  by

$$\omega = \frac{2\pi}{\tau}. \quad (4)$$

For this reason, the heating rate is not a constant value,

$$\frac{dT}{dt} = \beta_0 + A\omega \cos(\omega t). \quad (5)$$

As can be seen, we have to distinguish between the different ways of TMDSC operation depending on the magnitude of these three measuring parameters  $\beta_0$ ,  $A$ , and  $\omega$ : quasi-isothermal mode ( $\beta_0 = 0$ ), heating only mode ( $\beta_0 > A\omega$ ), heating-iso mode ( $\beta_0 = A\omega$ ), and heating-cooling mode ( $\beta_0 < A\omega$ ). The choice of the values of these three parameters determines the modes of TMDSC operation<sup>29</sup>. In practice, the use of one or another mode is applied without considering that depending on the sample subjected to one or another condition can be translated in detecting different processes or the same processes but with different signals.

The TMDSC method-1 and method-3 employ a heating-cooling mode ( $\beta_0 < A\omega$ ). The sinusoidal heating-cooling rate fluctuations take positive and negative

values in each period (Figure 1a and c). The method-2 was created with the aim of changing the operation modes of heating-cooling to heating-iso mode ( $\beta_0 = A\omega$ ), keeping the initial conditions employed in method-1. The values of  $\omega$  and  $\beta_0$  were kept and only the value of  $A$  was modified from 1°C to 0.16°C. As can be seen in Figure 1b, method-2 employs a heating-iso mode. The sinusoidal heating-cooling rate fluctuation takes only positives values.

## Results and discussion

Figure 2 and Table 2 show the DSC thermograms and the thermal parameter values obtained in each sample.

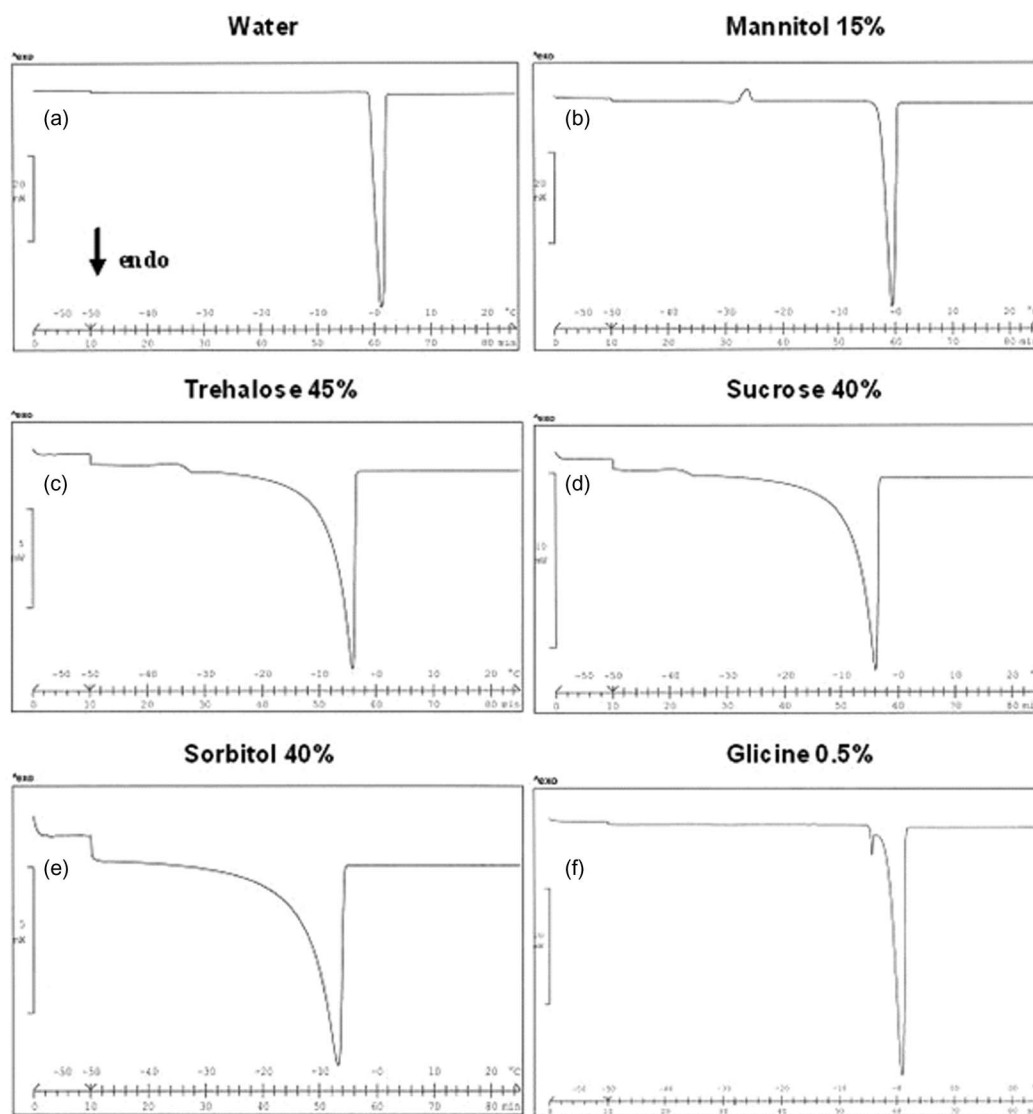


**Figure 2.** (a) DSC thermograms of distillate and deionized water, (b) mannitol aqueous solution at 15% (w/v), (c) trehalose aqueous solution at 45% (w/v), (d) sucrose aqueous solution at 40% (w/v), (e) sorbitol aqueous solution at 40% (w/v), and (f) glycine aqueous solution at 0.5% (w/v), respectively.

**Table 2.** Average values of calorimetric parameters of different samples of each TMDSC method used.

	DSC	TMDSC		
		Method-1	Method-2	Method-3
Distilled and deionized water				
$\Delta H_m$ (J/g)	$371 \pm 6.5$	$333 \pm 1.53$	$382 \pm 4.65$	$353 \pm 2.1$
$T_m$ (°C)	$0.3 \pm 0.04$	$0.87 \pm 0.11$	$0.2 \pm 0.02$	$-1.47 \pm 0.03$
Mannitol solution 15% (w/v)				
$\Delta H_m$ (J/g)	$392 \pm 2.7$	$313 \pm 0.85$	$359 \pm 5.82$	$335 \pm 1.95$
$T_m$ (°C)	$-1.55 \pm 0.06$	$-1.01 \pm 0.09$	$-1.65 \pm 0.007$	$-3.32 \pm 0.03$
$\Delta H_c$ (J/g)	$15.8 \pm 0.3$	$14.7 \pm 0.25$	$13.75 \pm 0.98$	$16.7 \pm 0.21$
$T_c$ (°C)	$-26.2 \pm 0.07$	$-27.1 \pm 0.06$	$-26.5 \pm 0.06$	$-27.9 \pm 0.20$
Trehalose solution 45% (w/v)				
$\Delta H_m$ (J/g)	$289 \pm 0.5$	$117 \pm 1.17$	$182 \pm 8.28$	$94 \pm 5.24$
$T_m$ (°C)	$-4.38 \pm 0.01$	$-4.41 \pm 0.01$	$-2.64 \pm 0.15$	$-4.81 \pm 0.08$
$T_g$ (°C)	$-34.2 \pm 0.4$	$-32.9 \pm 0.07$	$-32.5 \pm 0.04$	$-35.2 \pm 0.42$
Sucrose solution 40% (w/v)				
$\Delta H_m$ (J/g)	$298 \pm 2.9$	$125 \pm 0.9$	$129 \pm 0.30$	$79 \pm 1.53$
$T_m$ (°C)	$-4.25 \pm 0.04$	$-4.41 \pm 0.01$	$-4.63 \pm 0.10$	$-4.58 \pm 0.07$
$T_g$ (°C)	$-37.9 \pm 0.56$	$-37.13 \pm 0.9$	$-35.6 \pm 0.01$	$-39.7 \pm 1.73$
Sorbitol solution 40% (w/v)				
$\Delta H_m$ (J/g)	$260 \pm 0.06$	$84 \pm 0.7$	$108 \pm 0.40$	$14 \pm 0.3$
$T_m$ (°C)	$-7.02 \pm 0.04$	$-6.21 \pm 0.04$	$-6.65 \pm 0.15$	$-18.5 \pm 0.01$
Glycine solution 0.5% (w/v)				
$\Delta H_m$ (J/g)	$4.9 \pm 0.42$	$6.77 \pm 0.5$	$7.11 \pm 0.06$	$12.2 \pm 0.23$
$T_m$ (°C)	$-4.37 \pm 0.01$	$-1.74 \pm 0.5$	$-0.01 \pm 0.06$	$-3.94 \pm 0.02$
$\Delta H_m$ (J/g)	$313 \pm 25.12$	$233 \pm 1.05$	$124 \pm 1.65$	$268 \pm 2.0$
$T_m$ (°C)	$0.07 \pm 0.05$	$-0.51 \pm 0.01$	$0.53 \pm 0.02$	$-1.84 \pm 0.05$

$\Delta H_m$ , melting enthalpic difference;  $T_m$ , melting temperature;  $\Delta H_c$ , crystallization enthalpic difference;  $T_c$ , crystallization temperature;  $T_g$ , glass transition temperature.

The distilled and deionized water DSC thermogram (Figure 2a) shows an endothermic and narrow peak at  $0.3 \pm 0.04^\circ\text{C}$  which corresponds to the ice melt with an enthalpy difference ( $\Delta H$ ) of  $371 \pm 6.5$  J/g. This value is near to the bibliographic value for pure ice  $333.7$  J/g<sup>30,31</sup>.

In Figure 2b, the mannitol solution samples at 15% (w/v) in distilled and deionized water were analyzed. It shows an exothermic peak at  $-26.2 \pm 0.07^\circ\text{C}$  with an  $\Delta H$  of  $15.8 \pm 0.3$  J/g and a second endothermic and narrow peak at  $-1.55 \pm 0.06^\circ\text{C}$  with an  $\Delta H$  of  $333 \pm 2.7$  J/g. The first peak corresponds to a mannitol recrystallization, a process described in the literature that occurs between  $-25^\circ\text{C}$  and  $-30^\circ\text{C}$ . The other peak is due to the ice melt into a sugar solution, at a lower temperature of pure ice but with the same bibliographic  $\Delta H$  value<sup>32–34</sup>.

The DSC thermogram of trehalose solution samples at 45% (w/v), Figure 2c, shows a  $T_g$  at  $-34.2 \pm 0.4^\circ\text{C}$ , recently described in literature as the  $T_g$  of the maximally freeze concentrated solute<sup>35,36</sup> and an endothermic and wide peak with tail at  $-4.38 \pm 0.01^\circ\text{C}$  with a  $\Delta H$  of  $159 \pm 0.5$  J/g. Because of the presence of the sugar in the aqueous solution, the average melting temperature of the samples is below that of the pure ice and produces a

broad melting endotherm due to the melts of the ice into the concentrated sugar solution.

As trehalose solution thermograms, the DSC analysis of sucrose solutions at 40% (w/v), Figure 2d, shows a  $T_g$  at  $-37.9 \pm 0.6^\circ\text{C}$ <sup>37,35</sup> and an endothermic and broad peak with tail at  $-4.25 \pm 0.04^\circ\text{C}$  with a  $\Delta H$  of  $172 \pm 2.9$  J/g. As it was expected for the addition of a cryoprotectant to the water, the melting temperature and the  $\Delta H$  value of the aqueous mixture are lower than those of the pure ice are.

By DSC, sorbitol 40% (w/v) aqueous solution presents an endothermic and broad peak at  $-7.02 \pm 0.04^\circ\text{C}$  with an  $\Delta H$  of  $156 \pm 0.06$  J/g, values below those of pure ice (Figure 2e). Unlike trehalose and sucrose solutions already analyzed, this endotherm is detected with any previously detected phase transition due to the high water content<sup>38</sup>.

The 0.5% (w/v) glycine solution, the only solution used in this work with an amino acid as cryoprotectant, shows by means of DSC (Figure 2f) two enthalpic and very near peaks at  $-4.37 \pm 0.01^\circ\text{C}$  and  $0.07 \pm 0.05^\circ\text{C}$  with a  $\Delta H$  of  $4.9 \pm 0.42$  and  $311 \pm 25.1$  J/g, respectively. The first peak corresponds to the eutectic melting endotherm in addition to the second peak, the ice melting endotherm<sup>39</sup>. These values are lower than that obtained for the pure ice.

By TMDSC, distilled and deionized water heat flow signal changes its initial amplitude value in the melting area, because of the incorporation of an excess of heat flow characteristic of this process (Figure 3a). Only in method-1, there are at least four modulation cycles during the transitions of interest. The other methods employ insufficient cycles through the peak and this can be detrimental to the signal deconvolution process<sup>40,23</sup>. After the melt, the periodic applied function is recovered with higher amplitude than the initial value. In fact, the heat capacity is expected to be higher in the melted phase than in the solid crystalline phase<sup>24</sup>. This effect is checked by the construction of Lissajous figures for the three methods (Figure 4). This plot confirms the change in the modulated parameters applied, the amplitude in this case, before and after the event for the three methods employed. The distortion of the ellipse occurs with the melt and the eccentricity of the ellipse changes after it<sup>41,42,35</sup>. The enthalpy difference value obtained with method-1 is just like the bibliographic value for the pure ice<sup>30,31</sup>. In method-2 and method-3, this value increases. Except for method-3, the melting temperature was close to  $0^\circ\text{C}$ . Figure 5a shows how the  $C_{p \text{ in-phase}}$  evolution is in-phase with the melt as it is expected for a reversible transition.

For mannitol samples, the heat flow signal shows two peaks as they were detected by conventional DSC (Figure 3b): one due to the recrystallization of the sugar (exothermic peak) and other due to the melt of the ice into a sugar solution (endothermic peak). After each

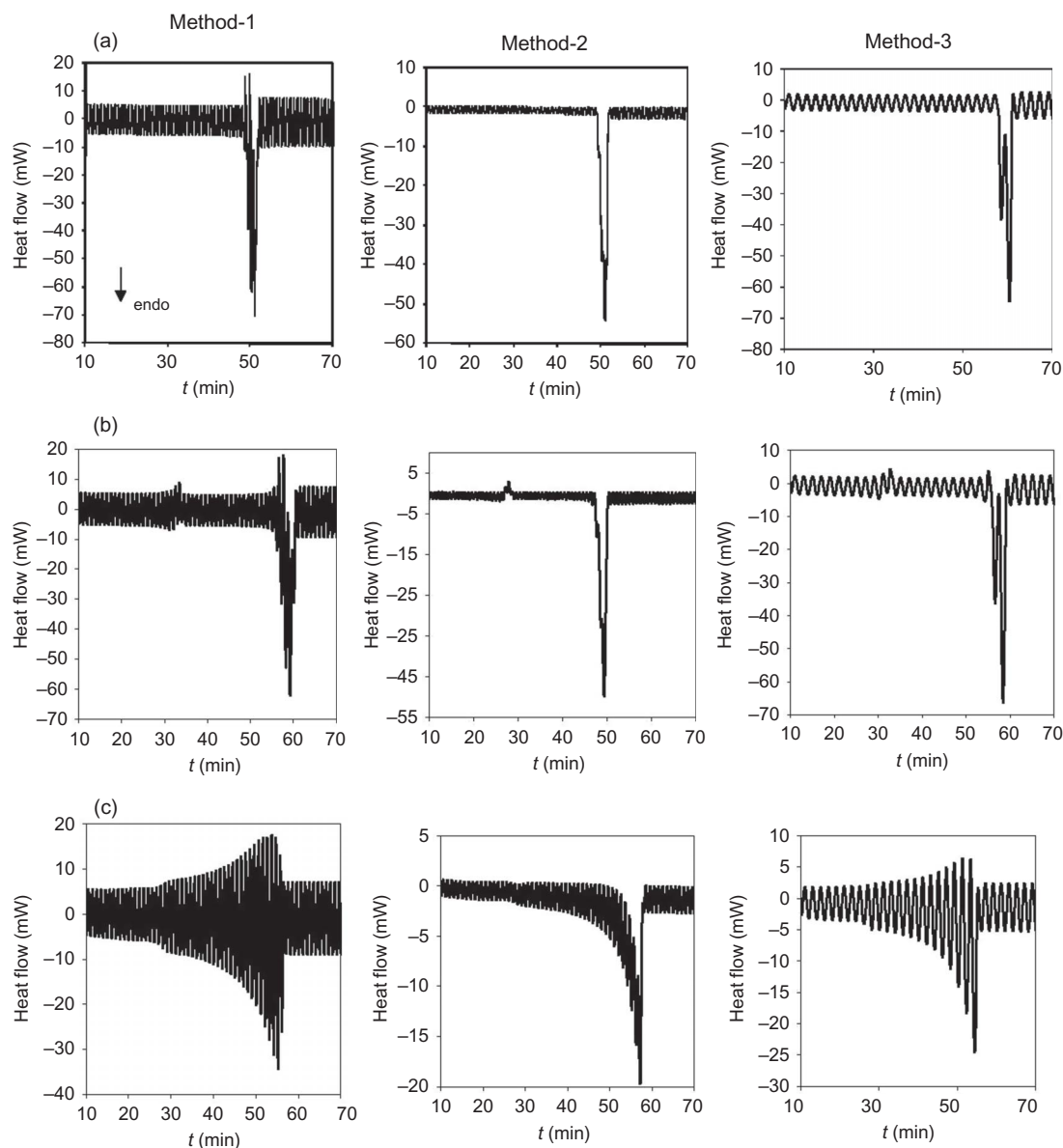


**Figure 3.** Heat flow evolution of (a) water, (b) mannitol 15% (w/v), and (c) trehalose 45% (w/v) in method-1, method-2, and method-3, respectively.

thermal event, the amplitude value increases like water samples. Because of the different calorimetric parameters used by each TMDSC method, the  $\Delta H$  average value of the melted sugar aqueous solution varies from 266 to 305 J/g. Likewise, the melting temperature gradually decreases like the cryoscopic decrease of the aqueous solution<sup>10</sup>, as it could be expected. This decrease was accentuated in method-3. The mannitol cold crystallization during the heating of the sample occurs at a temperature interval described in the literature ( $-25^{\circ}\text{C} \leftrightarrow -31^{\circ}\text{C}$ ) and with an enthalpy difference which changes with the sinusoidal method employed. The main disadvantage of this process occurs when mannitol is used in the formulation of drugs. During the sample conservation, the sugar could recrystallize and

expand the product with the consequent breakdown of the drug container<sup>32–34</sup>. The plot of  $C_p$  in-phase with time is shown in Figure 5b.

The heat flow and  $C_p$  in-phase evolution with the time of trehalose aqueous solution 45% (w/v) included in Figures 3c and 5c, respectively, was obtained by TMDSC. It shows the two process detected previously by conventional DSC: the  $T_g$  of the frozen sugar solution and the melt of its aqueous solution. The  $\Delta H$  value changes from the different TMDSC methods and it is different from the value obtained by conventional DSC. Except for method-2, the solution melting temperature is approximately the same. The  $T_g$  value determined for the sugar is in the interval between  $-32.5^{\circ}\text{C}$  and  $-35.0^{\circ}\text{C}$  as the literature points to<sup>35,36</sup>. The heat flow signals for

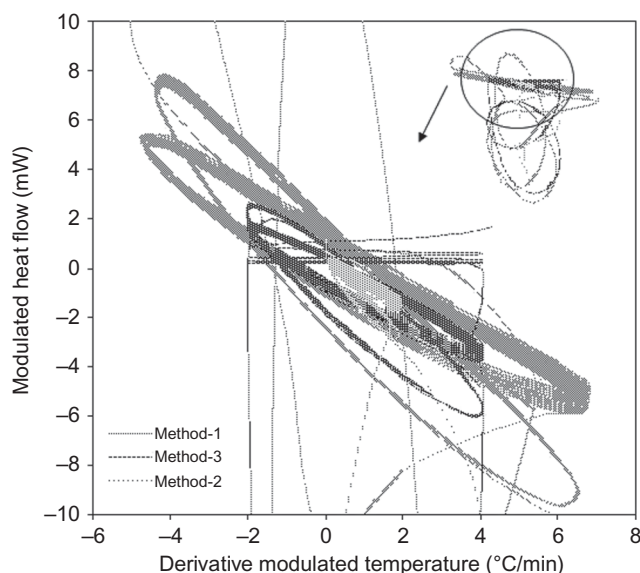


**Figure 4.** Lissajous figures for water samples in TMDSC method-1, method-2, and method-3.

all methods show an increase in its amplitude value from the  $T_g$  area to the melt with an increase in  $C_{p \text{ in-phase}}$  value, and it is recovered after the events but with a higher value than the former one.

Figure 5d shows the TMDSC  $C_{p \text{ in-phase}}$  evolution of sucrose 40% (w/v) aqueous solution samples. It was detected from the same events previously described by DSC: the sugar phase transition and the melt of the aqueous solution. The evolution of heat flow and  $C_{p \text{ in-phase}}$  signals are approximately the same as with trehalose samples, its values change from the first event up to the last one. The values of the  $T_g$  of the sugar detected in each TMDSC method are in the interval showed by the bibliography, approximately  $-36^\circ\text{C}$ <sup>43,44,38</sup> (see Table 2). The  $\Delta H$  values change from method-1 to method-3 at the same melting temperature than that detected by conventional DSC.

By TMDSC, the sorbitol samples at 40% (w/v) show the same event detected by conventional DSC, the melt of the aqueous solution, at a temperature interval of  $-6.2^\circ\text{C}$  to  $-18.5^\circ\text{C}$  with an  $\Delta H$  that changes from 8.43 to 50.3 J/g. Unlike trehalose and sucrose, the  $C_{p \text{ in-phase}}$  (Figure 5e) shows the change in its values in the area of the thermal event without any transition signal before the melt.

Figure 5f shows the  $C_{p \text{ in-phase}}$  evolution for glycine aqueous solution at 0.5 % (w/v). The  $C_p$  signal changes in the area of the melt. The melting temperature of the eutectic is higher than that detected by DSC with a  $\Delta H$  in the interval 4.9–12.2 J/g. For the ice melt, the detected temperature goes from about  $0^\circ\text{C}$  to  $-1.84^\circ\text{C}$  with a  $\Delta H$  lower than that calculated by conventional DSC.

As can be seen, DSC and TMDSC are able to detect the same processes which take place but with different resultant heat flow signals. Then, the values of the calorimetric parameters determined are different for every cryoprotectant's dissolution analyzed.

## Conclusions

The comparative determinations carried out by conventional DSC and TMDSC after freezing the samples indicate that the selection of the calorimetric parameters of each temperature program applied is crucial for the correct identification of thermal transitions and basic temperatures of each material or system to be studied. In our study, the TMDSC thermograms have confirmed the events previously detected by conventional DSC; trehalose, sucrose, and sorbitol have a less critical temperature of primary drying than the other samples because of the melting of ice into the sugar solution; in the case of trehalose and sucrose, it starts after the  $T_g$  of the frozen sugar solution.

Unlike DSC, the resultant heat flow signal in TMDSC changes with the values of the different measuring parameters used: the underlying heating-cooling rate ( $\beta_0$ ), the temperature fluctuation amplitude ( $A$ ), and the angular frequency modulation ( $\omega$ ). For this reason, the values of the calorimetric parameters determined are different if measured in a mode of heating-cooling or heating-iso. The TMDSC method-1 seems to be the most adequate combination of calorimetric parameters because of the higher number of cycles involved in each thermal event. The plot of Lissajous figures for each sample and method used shows the change in the calorimetric parameters at the event as a distortion of the ellipse and, in the end as a change in its eccentricity. The  $C_{p \text{ in-phase}}$  signal evolution represents the clearest way to check the reversibility of thermal events showed by the heat flow signal. In fact, the possibility of separating the reversible from the nonreversible thermal process by modulation of temperature program is an important option to take into account<sup>45</sup>, though for some materials or systems the TMDSC use contributes to have experimental difficulties and more complicate results to be understood than conventional DSC, depending on the type of event studied. This has an important role at the time of studying the way of interaction between these cryoprotectants substances and different types of drugs like proteins when its mixtures, as an instance, are frozen as a previous step of lyophilization. Because of that, it is basic to know the way to work with the thermal program depending on the process we want to detect and investigate.



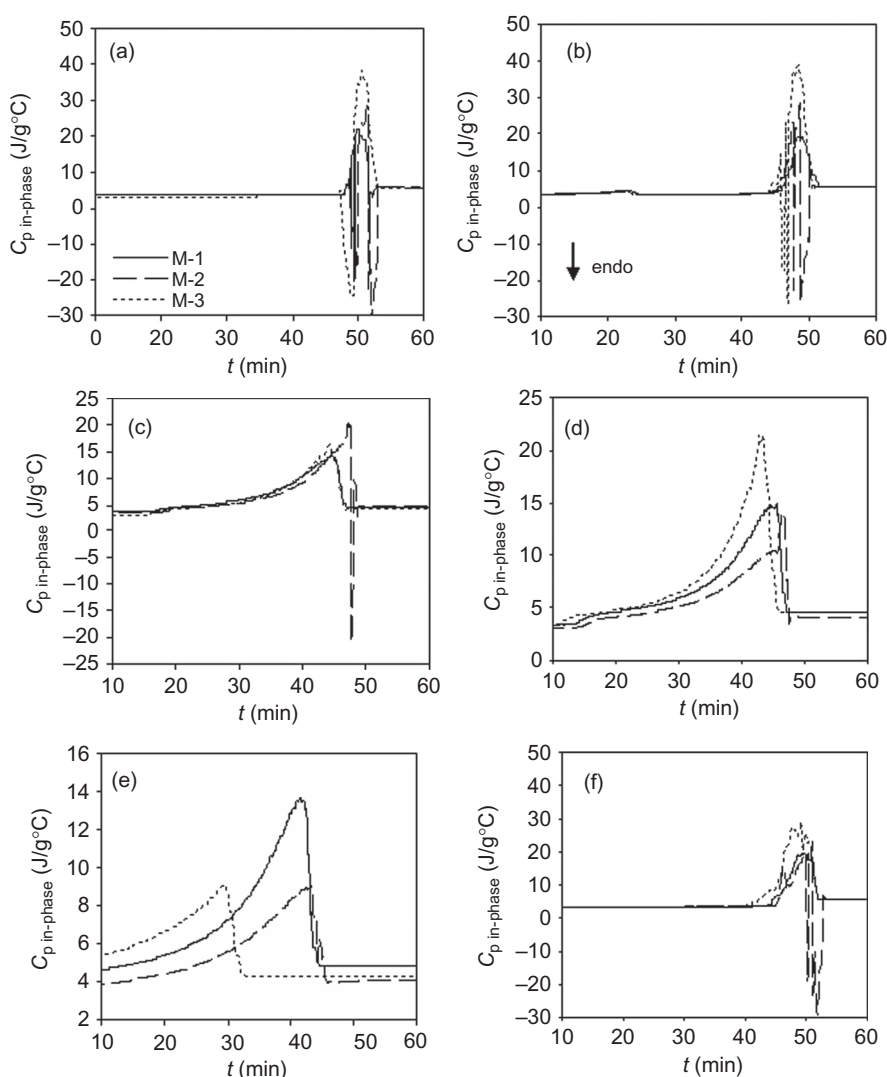


**Figure 5.**  $C_{p \text{ in-phase}}$  evolution with time for (a) water, (b) mannitol, (c) trehalose, (d) sucrose, (e) sorbitol, and (f) glycine samples, respectively.

## Declaration of interest

The authors report no conflicts of interest. The authors alone are responsible for the content and writing of this paper.

## References

1. Cappola ML. (2000). Freeze-drying concepts. In: MacNally, EJ, ed. Protein formulation and delivery. New York: Marcel Dekker, 159–99.
2. Caira MR, Alkhamis KA, Obaidat RM. (2004). Preparation and crystal characterization of a polymorph, a monohydrate, and an ethyl acetate solvate of the antifungal fluconazole. *J Pharm Sci*, 93:601–11.
3. Chao RS, Vail KC. (1987). Polymorphism of 1,2-dihydro-6-neopentyl-2-oxonicotinic acid: Characterization, interconversion, and quantitation. *Pharm Res*, 4:429–32.
4. Cheng W-T, Lin S-Y, Wang S-L. (2008). Differential scanning calorimetry with curve-fitting program used to quantitatively analyze the polymorphic transformation of famotidine in the compressed compact. *Drug Dev Ind Pharm*, 34:1368–75.
5. Hamdani J, Moes AJ, Amighi K. (2003). Physical and thermal characterisation of Precirol and Compritol as lipophilic glycerides used for the preparation of controlled-release matrix pellets. *Int J Pharm*, 260:47–57.
6. Ibrahim HG, Pisano F, Bruno A. (1977). Polymorphism of phenylbutazone: Properties and compressional behavior of crystals. *J Pharm Sci*, 66:669–73.
7. Telang C, Suryanarayanan R, Yu L. (2003). Crystallization of D-mannitol in binary mixtures with NaCl: Phase diagram and polymorphism. *Pharm Res*, 20:1939–45.
8. Hottot A, Daoussi R, Andrieu J. (2006). Thermophysical properties of aqueous and frozen states of BSA/water/Tris systems. *Int J Biol Macromol*, 38:225–31.
9. Kurkuri MD, Aminabhavi TM. (2004). Poly(vinyl alcohol) and poly(acrylic acid) sequential interpenetrating network pH-sensitive microspheres for the delivery of diclofenac sodium to the intestine. *J Control Release*, 16:9–20.



10. Lahiani-Skiba M, Barbot C, Bounoure F, Joudieh S, Skiba M. (2006). Solubility and dissolution rate of progesterone-cyclodextrin-polymer systems. *Drug Dev Ind Pharm*, 32:1043-58.
11. Lin SY, Chen KS, Teng HH. (1999). Protective colloids and polylactic acid co-affecting the polymorphic crystal forms and crystallinity of indomethacin encapsulated in microspheres. *J Microencapsul*, 16:769-76.
12. Hawe A, Friess W. (2006). Impact of freezing procedure and annealing on the physico-chemical properties and the formation of mannitol hydrate in mannitol-sucrose-NaCl formulations. *Eur J Pharm Biopharm*, 64:316-25.
13. Jovanovic N, Bouchard A, Hofland GF, Witkamp GF, Crommelin DJ, Jiskoot W. (2006). Distinct effects of sucrose and trehalose on protein stability during supercritical fluid drying and freeze-drying. *Eur J Pharm Sci*, 27:336-45.
14. Cueto M, Dorta MJ, Munguía O, Llabrés M. (2003). New approach to stability assessment of protein solution formulations by differential scanning calorimetry. *Int J Pharm*, 252:159-66.
15. Kurganov BI, Lyubarev AE, Sanchez JM, Shnyrov VL. (1997). Analysis of differential scanning calorimetry data for proteins. Criteria of validity of one-step mechanism of irreversible protein denaturation. *Biophys Chem*, 69:125-35.
16. Mukaiyama A, Haruki M, Ota M, Koga Y, Tacaño K, Kanaya S. (2006). A hyperthermophilic protein acquires function at the cost of stability. *Biochemistry*, 45:12673-9.
17. Reading M. (1993). Modulated differential scanning calorimetry—A new way forward in materials characterization. *Trend Polym Sci*, 1:248-53.
18. Abdelwahed W, Degobert G, Stainmesse S, Fessi H. (2006). Freeze-drying of nanoparticles: Formulation, process and storage considerations. *Adv Drug Deliv Rev*, 58:1688-713.
19. Aldén M, Hillgren A. (1998). Investigation of aqueous solutions by modulated temperature differential scanning calorimetry. *Thermochim Acta*, 311:51-60.
20. Keymolen B, Ford JL, Powell MW, Rajabi-Siahboomi AR. (2003). Investigation of the polymorphic transformations from glassy nifedipine. *Thermochim Acta*, 397:103-17.
21. Royall PG, Craig DQ, Doherty C. (1999). Characterisation of moisture uptake effects on the glass transitional behaviour of an amorphous drug using modulated temperature DSC. *Int J Pharm*, 192:39-46.
22. Craig DQM. (1999). Pharmaceutical applications of modulated temperature calorimetric techniques. *Int J Pharm*, 192(1):1-103.
23. Verdonck E, Schaap K, Thomas LC. (1999). A discussion of the principles and applications of modulated temperature DSC (TMDSC). *Int J Pharm*, 192:3-20.
24. Jiang Z, Imrie CT, Hutchinson JM. (2002). An introduction to temperature modulated differential scanning calorimetry (TMDSC): A relatively non-mathematical approach. *Thermochim Acta*, 387:75-93.
25. Boottom R. (1999). The role of modulated temperature differential scanning calorimetry in the characterisation of a drug molecule exhibiting polymorphic and glass forming tendencies. *Int J Pharm*, 192:47-53.
26. Lai HL, Pitt K, Craig DQM. (2010). Characterisation of the thermal properties of ethylcellulose using differential scanning and quasi-isothermal calorimetric approaches. *Int J Pharm*, 386:178-84.
27. Qi S, Gryczke A, Belton P, Craig DQM. (2008). Characterisation of solid dispersion of paracetamol and EUDRAGIT® E prepared by holt-melt extrusion using thermal, microthermal and spectroscopic analysis. *Int J Pharm*, 354:158-67.
28. Schubnell M, Schawe JEK. (2001). Quantitative determination of the specific heat and the glass transition of moist samples by temperature modulated differential scanning calorimetry. *Int J Pharm*, 217:173-81.
29. Höhne GWF, Hemminger WF, Flammersheim H-J. (2000). Theoretical fundamentals of differential scanning calorimeters. In: *Differential scanning calorimetry*. Berlin: Springer, 31-63.
30. Haensler M, Maedler B, Richter W, Volke F. (2000). Investigation of frozen protease-catalyzed peptide synthesis systems—A differential scanning calorimetry and electron microscopy approach. *J Mol Catal B Enzym*, 9:91-95.
31. Rosilio V, Madelmont G, Akiyoski K, Sunamoto J, Baszkin A. (1994). Thermal behaviour of hydrated dimyristoyl/phosphatidylcholine/cholesteryl-pullulan mixtures. *J Colloid Interface Sci*, 162:418-24.
32. Kett VL, Fitzpatrick S, Cooper B, Craig DQM. (2003). An investigation into the subambient behavior of aqueous mannitol solutions using differential scanning calorimetry, cold stage microscopy, and X-ray diffractometry. *J Pharm Sci*, 92:1919-29.
33. Williams NA, Dean T. (1991). Vial breakage by frozen mannitol solutions: Correlation with thermal characteristics and effect of stereoisomerism, additives and vial configuration. *J Parenter Sci Technol*, 45:94-100.
34. Williams NA, Lee Y, Polli GP, Jennings TA. (1986). The effects of cooling rate on phase transitions and associated vial breakage in frozen mannitol solutions. *J Parenter Sci Technol*, 40:135-41.
35. Sacha GA, Nail SL. (2009). Thermal analysis of frozen solutions: Multiple glass transition in amorphous systems. *J Pharm Sci*, 98:3397-405.
36. Wu J, Reading M, Craig DQM. (2008). Application of calorimetry, sub-ambient atomic force microscopy and dynamic mechanical analysis to the study of frozen aqueous trehalose solutions. *Pharm Res*, 25:1396-404.
37. Goff HD, Verespej E, Jermann D. (2003). Glass transitions in frozen sucrose solutions are influenced by solute inclusions within ice crystals. *Thermochim Acta*, 399:43-55.
38. Talja RA, Roos YH. (2001). Phase and state transition effects on dielectric, mechanical, and thermal properties of polyols. *Thermochim Acta*, 380:109-21.
39. Chongprasert S, Knopp SA, Nail SL. (2001). Characterization of frozen solutions of glycine. *J Pharm Sci*, 90:1720-8.
40. Tang C-H, Choi S-M, Ma C-Y. (2007). Study of thermal properties and heat-induced denaturation and aggregation of soy proteins by modulated differential scanning calorimetry. *Int J Biol Macromol*, 40:96-104.
41. Baroni AF, Sereno AM, Hubinger MD. (2003). Thermal transitions of osmotically dehydrated tomato by modulated temperature differential scanning calorimetry. *Thermochim Acta*, 395:237-49.
42. Hill VL, Craig DQM, Feely LC. (1999). The effects of experimental parameters and calibration on TMDSC data. *Int J Pharm*, 192:21-32.
43. Bhandari B, Roos Y. (2003). Dissolution of sucrose crystals in the anhydrous sorbitol melt. *Carbohydr Res*, 338:361-7.
44. Chang L, Milton N, Rigsbee D, Mishra D, Tang X, Thomas L, et al. (2006). Using modulated DSC to investigate the origin of multiple thermal transitions in frozen 10% sucrose solutions. *Thermochim Acta*, 444:141-7.
45. Rodríguez-Cabello JC, Reguera J, Alonso M, Parker TM, McPherson DT, Urry DW. (2004). Endothermic and exothermic components of an inverse temperature transition for hydrophobic association by TMDSC. *Chem Phys Lett*, 388:127-31.

Copyright of Drug Development & Industrial Pharmacy is the property of Taylor & Francis Ltd and its content may not be copied or emailed to multiple sites or posted to a listserv without the copyright holder's express written permission. However, users may print, download, or email articles for individual use.